

## EFFECT OF SOLUTION CONCENTRATION ON SOME OPTICAL PROPERTIES OF INDIUM OXIDE DOPED WITH $\text{SnO}_2$ THIN FILMS PREPARED BY CHEMICAL SPRAY PYROLYSIS TECHNIQUE

Yasmeen Z. Dawood\*, Majid H. Hassoni\*, Mohamad S. Mohamad\*\*

\* University of Mustansiriyah, Collage of education, Baghdad, Iraq.

\*\* University of Technology, Applied science department, Baghdad, Iraq.

---

**ABSTRACT:** *The aim of this research is to study the role of concentration variations on precursor solution of  $\text{SnO}_2$  doped  $\text{In}_2\text{O}_3$  ( $\text{In}_2\text{O}_3:\text{Sn}$ ) thin films which has been prepared by spray pyrolysis technique. The change in doping concentration corresponds to changes observed in the XRD spectra, where crystal orientation of  $\text{In}_2\text{O}_3:\text{SnO}_2$  thin films was (211) and (222). All of the  $\text{In}_2\text{O}_3:\text{SnO}_2$  thin films have kept their sharp ultra violet absorption edge, but the transparency in visible spectra region decreases as the molarities in precursor solution increase. These data prove the capability of spray pyrolysis as a viable technique in preparing TCO materials and so, fully transparent CMOS-like devices.*

**KEYWORDS:** Indium tin oxide, Spray pyrolysis, Optical and Structure properties.

---

### INTRODUCTION

Indium Oxide is a direct wide band gap ( $> 3.5$  eV) n-type semiconductor which makes the transmission window between wavelengths 300 nm and 1500 nm, depending on the processing conditions. At short wavelengths (high energies - UV range) electron interband transitions from the valence to unoccupied states in the conduction band limit the transmission up to the band gap [1-4]. For long wavelengths (low energies - IR range), light is reflected because of the quasi-free electron plasma. Thus, the wavelength cutoff in the IR depends on the charge carrier density. An indirect band of 2.62 eV has been calculated by Weiher et al. [5]. This carrier density is related to the oxygen stoichiometry, where, in the ideal case, each doubly charged oxygen vacancy contributes two free electrons and to the doping element when the latter is present. These defects create an impurity band that overlaps the conduction band, thereby creating a “degenerate” semiconductor (i.e. its behavior approximates that (semi-)metals. Increasing the carrier density also leads to a widening of the band gap known as the Burstein-Moss effect. This effect competes with many body effects (electron-electron interactions) which tend to decrease the band gap. However, it is a double edged sword: doubly charged O vacancies and singly charged Sn on an In site reduce the mobility of charge carriers via ionised impurity scattering. In addition, oxygen vacancies play an important role in all processes related to solid-state diffusion, including recrystallization, grain growth, sintering and phase transformations. They are electrically charged and can be associated with dopant atoms to form neutral or charged complexes [6-8].

A transparent conducting oxide is a semiconducting material combining high conductivity and optical transparency. Within the transparent conducting oxides category, Indium Tin Oxide (ITO) is still the most widely used. The physical characteristics of semiconductors are

determined both by the properties of the host crystal and by the presence of impurities and crystalline defects [9, 10]. Dopant impurities, which typically substitute for a host crystal atom, introduce electronic states in the bandgap close to the valence and conduction band edges and thus determine the type and conductivity of the material. These so-called shallow level defects enable a wide range of semiconductor properties. However, crystal lattice defects and other impurities, which introduce electronic states deeper in the bandgap and are referred to as deep level defects, also modify the properties of the semiconductor and thus may make a semiconductor unsuitable for its intended applications. It is then necessary to control carefully the deposition process to adjust the required properties [11-14].

Tin-doped indium oxide (ITO) thin films have been commonly used for opto-electronic applications due to low resistivity, high transmittance, and good etching properties. Many researchers have reported the use of spectroscopic ellipsometry for measuring optical constants (refractive index,  $n$ , and extinction coefficient,  $k$ ) of ITO thin films. Several dispersion relations such as the Cauchy models or the Lorentz oscillator models or the Drude models have been used to describe the optical constants of ITO thin films [15].

Numerous works for indium tin oxide (ITO) film synthesis have been performed for improving conductivity as well as high transparency as a transparent conductive oxide (TCO) material for transparent electrode application on glass substrate [16]. The ITO thin films commonly fabricated by different techniques such as Spray Pyrolysis techniques [17], Sputtering techniques [1, 8, 9], Evaporation techniques [10], electron beam, Sol-gel method [11] and Pulsed Laser Deposition of ITO thin films [6]. In this study ITO thin film deposited on glass substrate at lower deposition. In this study, different doping concentration of ITO films deposited on glass substrates have been prepared by spray pyrolysis method using low deposition temperature with different deposition conditions. The structural and optical properties of the obtained films depending on deposition parameters, such as doping concentration have been investigated.

## EXPERIMENTAL WORK

In this, research  $\text{In}_2\text{O}_3:\text{SnO}_2$  thin films were deposited by SP technique on glass substrates. The carrier gas used in all the experiments was filtered air, which was supplied by an air compressor. The distance among substrate and nozzle has been fixed at 30 cm. To prevent precipitation, a few droplets of acetic acid were added to precursor solution. Air flow rate was 18 Lit/min. The technique of active spray pyrolysis from aqueous  $\text{InCl}_3 \cdot 4\text{H}_2\text{O}$  solution was used for deposition of ITO films. A schematic of the experimental apparatus used for deposition of metal oxide films was shown schematically in Ref. [5]. Variations in deposition parameters such as precursor concentration (2% - 6%), temperature of pyrolysis ( $T=573\text{K}$ ), and volume of sprayed solution 20 ml were used for controlling the structure of the deposited films. The flow rate of sprayed solution was 0.15 ml/s for all experiments. The film thickness ( $d$ ) was varied in the range of 10–450 nm.

The optical properties of ITO films were analyzed by UV/VIS/ NIR spectrometer (Varian, Cary5000) and X-ray diffraction system (RIGAKU-12KW).

## RESULTS AND DISCUSSION

The optical transmittance in the UV-VIS region of the ITO films changes with different doping concentration was shown in Fig. 1. As conductivity increase, the optical transmittance of ITO thin films increase with doping concentration. Therefore, optical transmittance is also closely related to doping concentration, which is associated with free electrons in ITO films. We conclude that many electrons or disordered lattice structures in ITO films are scattered by incident light, thus reducing the transparency of the ITO thin film.

The transmittance of ITO film is also greatly improved as shown in Fig. 1. The ITO film deposited at 2% doping concentration reaches to a range of 87% of highest transmittance at the visible range from 400nm to 800nm, which is supposed to the increment of crystallization. However, the optical property becomes to reduce for the films synthesized with increasing doping concentration to 4%. This implies that  $\text{SnO}_2$  addition in solution of spraying plays an important role in effective ionization of indium and oxygen ion species and thereby enhancing energy delivery to the substrate surface for the nucleation and growth of ITO crystallites at low temperature less than 573K. This means the degree of free carrier absorption is significantly reduced in ITO films presumably due to the high  $\mu$ . From the plot of absorption  $\alpha$  vs photon energy  $h\nu$  Fig. 2, the optical band gap of the films was estimated. A maximum value of 3.9 eV obtained for the films ITO with 4% doping concentration was decreased to the range of 3.7 - 3.74 eV for variation Sn doping levels. The increasing in  $E_g$  with increasing doping concentration can be explain as an energy band widening effect resulting from the increase in the Fermi levels in the conduction band of degenerated semiconductors.

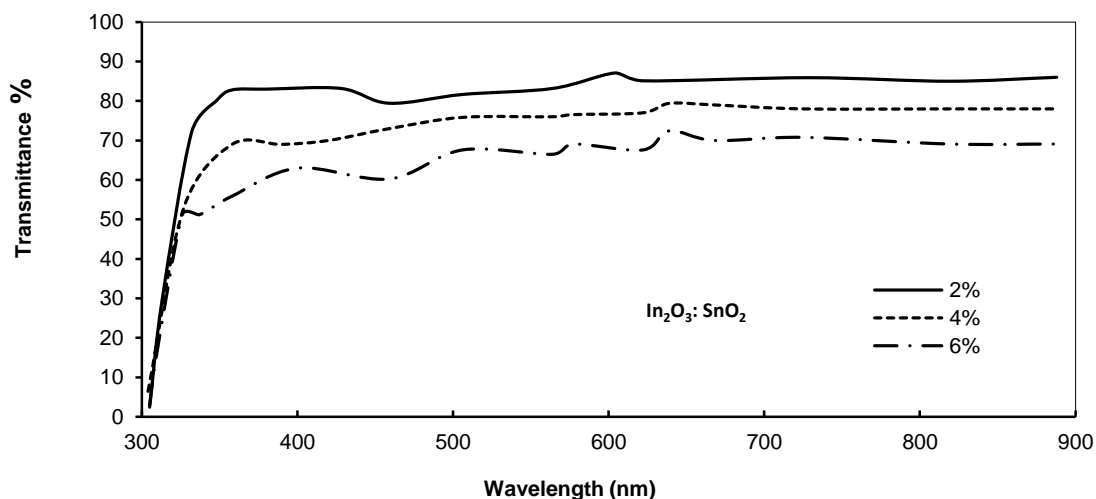


**Figure 1.** Influence of the fabrication doping concentration  $C_p$  on the ITO transmittance.

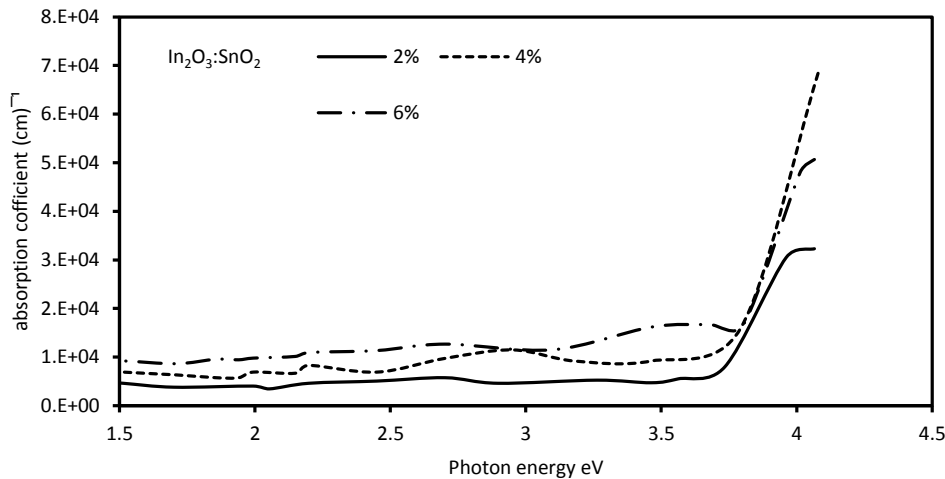


**Figure 2.**  $\alpha$  vs  $h\nu$  plot for ITO thin film with different Sn doping concentration.

Refraction of a medium can be described by a single quantity: the complex refractive index  $n_c$ :  $n_c = n + ik$ .  $n$  is the refractive index and it describes the velocity of light  $v$  in the medium since  $n = c/v$  where  $c$  is the speed of light in vacuum.  $k$  is called the extinction coefficient and it describes the attenuation of light wave  $\lambda$  as it goes through a material.  $k$  is directly related to the absorption coefficient  $\alpha$  of a medium. It was shown that [11, 18]:

$$\alpha = \frac{4\pi k}{\lambda} \quad \dots\dots\dots 1$$

Fig. 3(a) and (b) presents the spectra of the refractive indices and the extinction coefficients of the ITO films deposited at 300 C different doping concentrations (2%, 4% and 6%). The compared optical constants were extracted from the upper ITO layer for all the samples. Within the doping concentration range of this experiment, more doping rate resulted in higher refractive indices and lower extinction coefficients. Higher doping rate resulted in lower refractive indices. The changes in extinction coefficients are quite different between the visible range (about 400–700 nm) and the near infrared region (above 700 nm). In the visible range, the extinction coefficients were higher for higher doping rate conditions. However, in the near infrared region, higher doping rate led to larger extinction coefficients.

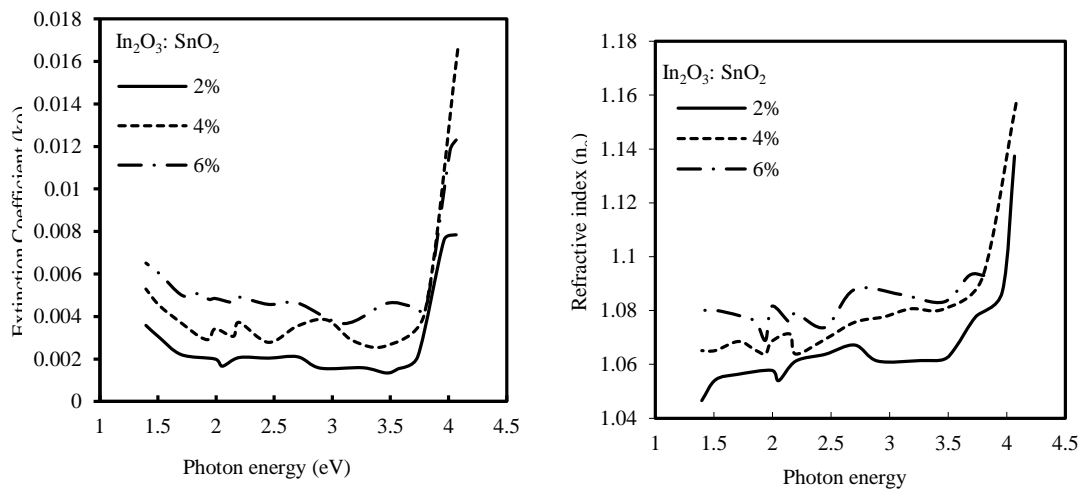


**Figure 3.** Variation of a) extinction coefficient b) refractive index with the photon energy.

Fig. 4 shows the XRD patterns of the ITO samples with different doping concentration. The ITO samples were deposited at 573K substrate temperature. The ITO samples deposited under this condition had mixed orientations. We have elaborately discussed the development of ITO film texture during spray pyrolysis deposition. It has been observed that the (222) and (211) preferential orientation is highly dominant at the initial growth stage for any deposition condition. This is due to the fact that during the nucleation stage of ITO thin films, indium atoms on substrate are likely to aggregate into densely packed (211) planes which are close to (222) planes in bixbyite structure. But the dominant nature changed from (222) and (211) when there is an increase in substrate temperature and also due to an increase in film thickness. The degree of orientation of the (400) plane is expected to be dependent on the mobility of ad atoms on the substrate. In our case, the deposition took place at room temperature which must have limited the ad atom mobility and the films are amorphous at the as-deposited conditions. Therefore we observe a (222) preferential orientation to be dominant in all the ITO films deposited at doping concentration 2% to 6%. In addition, none of the spectra corresponding to higher annealing temperatures indicates any characteristic peaks of Sn, SnO, SnO<sub>2</sub>, which indicates that the Sn atoms are probably incorporated substitutionally into the In<sub>2</sub>O<sub>3</sub> lattice.

Low intensity and a broad diffraction peak were identified, corresponding to an incipient crystallization of the ITO in the In<sub>2</sub>O<sub>3</sub> (211)-oriented structure and other peaks, such as (200), (222), (400) and (332) of In<sub>2</sub>O<sub>3</sub> and SnO<sub>2</sub>. As the doping concentration increased, the intensity and narrowness of the (222) diffraction peak increased, indicating growth of the (222) oriented crystallites; other diffraction peaks appeared for crystallites with other orientations. The full width at half maximum (FWHM) of the (222) oriented diffraction peak decreased as doping concentration increased (inset in table 1). An estimation of the grain size of the polycrystalline ITO film was obtained from the broadening of the XRD peaks according to the Scherrer's formula [15, 19]:

$$D = \frac{0.9\lambda}{\beta \cos\theta} \quad \dots\dots\dots 2$$

Where  $D$  is the grain size,  $\lambda$  is the wavelength of the Cu-K $\alpha$  radiation used ( $\lambda=1.5405 \text{ \AA}$ ),  $\beta$  is experimentally observed diffraction peak width at half-maximum intensity (FWHM),  $\theta$  is the Bragg angle. For the fabrication of good quality thin film to use in optical devices, it is necessary to reduce the surface roughness and dislocation density of the ITO film. So the value of the dislocation density ( $\delta$ ) which gives the number of defects in the film was calculated from the average values of the crystallite size  $D$  by the relationship [17]:

$$\delta = \frac{1}{D^2} \quad \dots\dots\dots 3$$

The ( $hkl$ ) plane, FWHM value, grain size ( $D$ ) and dislocation density ( $\delta$ ) values of ITO thin film are listed in Table 1.

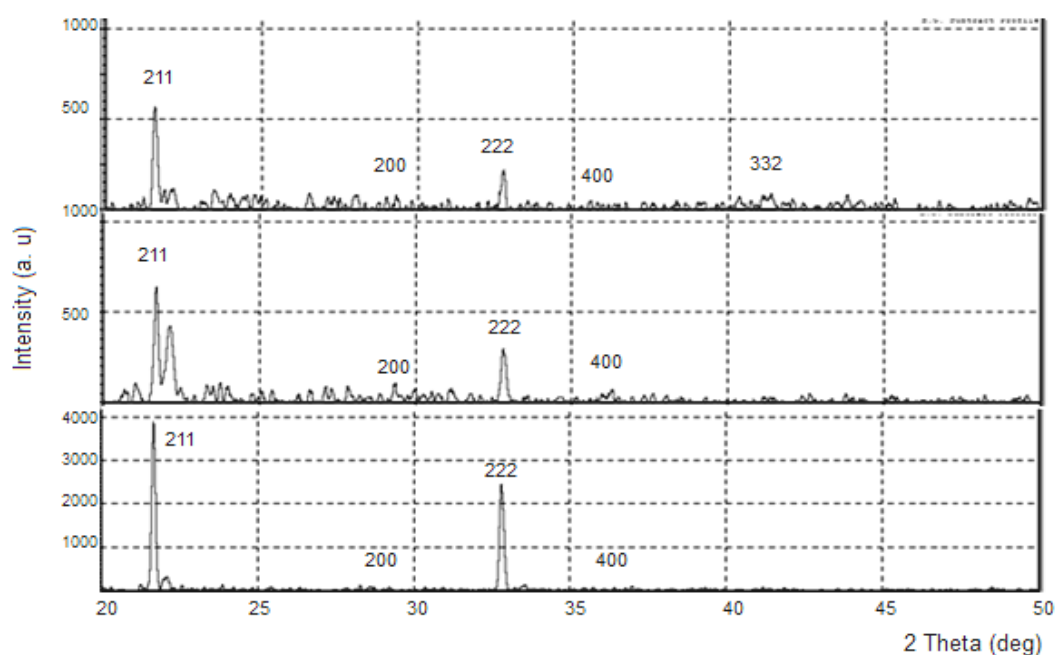


**Figure 4.** X-ray diffraction pattern of ITO thin films with a) 2%, b) 4% and c) 6% doping concentration

**Table 1.** (hkl) plane, FWHM, grain size (D) and dislocation density ( $\delta$ ) value of ITO thin films.

Doping concentration	(hkl)	Grain size (nm)	FWHM (deg)	Intensity ( $I/I_0$ )	d ( $\text{\AA}$ )	$\delta \times 10^{-4} (\text{nm})^{-2}$
2%	211	49	0.163	100	4.1	4.16
	200		0.11	17	3.1	
	222		0.08	14	2.8	
4%	211	55	0.14	100	4	3.3
	200		0.08	19	3.2	
	222		0.07	18	2.7	
6%	211	64	0.06	100	4	2.4
	200		0.06	4	3.1	
	222		0.12	72	2.7	

## CONCLUSION

ITO thin films with high transparency are deposited on glass substrate by the spray pyrolysis experimental technique. The films have been studied in detail as a function of the content of Sn ranging from 2% to 6%. The XRD studied confirmed polycrystalline films having a cubic bixbyite structure. The average transmittance 500-900 nm is higher than 87%. The obtained wide spectra range of transmittance suggests that the deposited ITO films could be utilized in the optoelectronic device where high transmittance is demanded.



**REFERENCES**

1. Ali, M. K. M., Ibrahim, K., Osama, S. H., Eisa, M. H., Faraj, M.G. and Azhari, F., (2011), "*Deposited Indium Tin Oxide (ITO) Thin films by DC magnetron sputtering on polyethylene terephthalate substrate (PET)*", Rom. Journ. Phys. 56 5–6 730–741
2. Giusti, G. (2011), "*Deposition and Characterisation of Functional ITO Thin Films*", A thesis submitted to The University of Birmingham for the degree of Doctor of philosophy School of Metallurgy and Materials, 2011.
3. Montesdeoca, S., Jimenez E. R., Marrero, N., Gonzz B. D., Borchert D., Guerrero R. L., (2010), "*XPS characterization of different thermal treatments in the ITO–Si interface of a carbonate-textured monocrystalline silicon solar cell*", Nuclear Instruments and Methods in Physics Research B 268 374–378.
4. Qiumei, B., Xiaoming, Y., Baozhen, Z., Zenghu, Ch. and Shuting, L., (2013), "*Femtosecond laser ablation of indium tin-oxide narrow grooves for thin film solar cells*" Optics & LaserTechnology 45 395–401.
5. Sung, J., Hong, Jong, W. K., Jae, W. L., Good, S. Ch. and Minoru, I. (2010), "*Characteristics of Printed Thin Films Using Indium Tin Oxide (ITO) Ink*", Materials Transactions 51 10 1905–1908.
6. Yoon, H. T., Ki, B. K., Hyoung, G. P., Kwang, H. L. and Jong, R. L. (2002), "*Criteria for ITO (indium–tin-oxide) thin film as the bottom electrode of an organic light emitting diode*" Thin Solid Films 411 12–16.
7. Shui, Y. L., (2010), "*Characterization and optimization of ITO thin films for application in heterojunction silicon solar cells*", Thin Solid Films 518 S10–S13.
8. Yeon, S. J., (2004), "*Spectroscopic ellipsometry studies on the optical constants of indium tin oxide films deposited under various sputtering conditions*", Thin Solid Films 467 36–42.
9. Chang, S. M. and Jeon G. H., (2008), "*Low temperature synthesis of ITO thin film on polymer in Ar/H<sub>2</sub> plasma by pulsed DC magnetron sputtering*", Thin Solid Films 516 6560–6564.
10. Pate, N.G., Pate, P.D., Vaishnav, V.S., (2003), "*Indium tin oxide (ITO) thin film gas sensor for detection of methanol at room temperature*", Sensors and Actuators B 96 180–189.
11. Davood, R., Ahmad, K., Hamid, Reza F., Amir, S. and Hassan, R., (2007), "*Surface characterization and microstructure of ITO thin films at different annealing temperatures*", Applied Surface Science 253 9085–9090.
12. Zhanlai, D., Cunran A., Qiang L., Zhezhe, H., Jianqiang, W., Haibo, Q., and Fangjuan Q., (2010), "*Preparation of ITO Nanoparticles by Liquid Phase Coprecipitation Method*", Journal of Nanomaterials Article ID 543601, 5 pages
13. Artorn, P., Mati, H. and Pichet, L., (2009), "*Songklanakarin Influence of oxygen flow rate on properties of indium tin oxide thin films prepared by ion-assisted electron beam evaporation*", J. Sci. Technol. 31 5 577–581.
14. Balasundaraprabhu, R. Monakhov, E.V., Muthukumarasamy, N., Nilsen, O., Svensson, B.G., (2009), "*Effect of heat treatment on ITO film properties and ITO/p-Si interface*", Materials Chemistry and Physics 114 425–429.
15. Joseph, J. P., Ramamurthy, S., Subramanian, B., Sanjeeviraj, C. and Jayachandran, M., (2002), "*Spray pyrolysis growth and material properties of In<sub>2</sub>O<sub>3</sub> films*", Journal of Crystal Growth 240 142–151.

16. Clewa, W., Ow, Y., Yuzo, Sh. and David, C. P., (2000), “*Interfacial stability of an indium tin oxide thin film deposited on Si and Si<sub>0.85</sub>Ge<sub>0.15</sub>*”, Jour. Of Appl. Phys. 88 5 15.
17. Pla, J. , Tamasi, M. , Rizzoli, R. , Losurdo, M. , Centurioni, E. , Summonte, C. and Rubinelli, F. , (2003), “ *Optimization of ITO layers for applications in a-Si<sub>1-x</sub>C<sub>x</sub>-Si heterojunction solar cell*”, Thin Solid Films 425 185–192.